

## A FSS WITH STABLE PERFORMANCE UNDER LARGE INCIDENT ANGLES

Tao Ma<sup>1</sup>, Hang Zhou<sup>2, \*</sup>, Yuan Yang<sup>2</sup>, and Bo Liu<sup>2</sup>

<sup>1</sup>College of Equipment Management and Security Engineering, Air Force Engineering University, Xi'an 710051, China

<sup>2</sup>Air Traffic Control and Navigation College, Air Force Engineering University, Xi'an 710051, China

**Abstract**—In this paper, we propose a novel frequency selective surface (FSS) with stable performance under large incident angles. The FSS is composed of hexagon metallic lines and hexagon patches. Using such a hexagon arrangement, the periodicity size could be miniaturized and thus the FSS unit cell is compact. The composite FSS has an excellent stability under large incident angles. In the passband 10.58–11.06 GHz, the insertion loss is still less than  $-1$  dB for both *TE* and *TM* polarizations, even under incident angle up to 85 degree. Both the design procedure and experimental results of the novel FSS are presented and discussed.

### 1. INTRODUCTION

Frequency selective surfaces (FSSs) are one- or two-dimensional planar periodic arrays of metallic patches or slots that function as bandstop or bandpass filters. For more than four decades, FSSs have been attractive because of their comprehensive applications, such as subreflectors, polarizers, flters, band-pass hybrid radomes [1–3]. Compared with conventional filters, frequency responses of FSSs are dependent not only on frequency but also on incident angle and polarizations of incident electromagnetic waves. It is required that FSS provide stable performance for both various incidence angles and different polarizations within its operating frequencies.

An important application of FSS is hybrid-radomes for radar cross-section (RCS) reduction [4, 5]. For an airborne FSS radome, to the nose cone, the incident angles can be very large even to

---

*Received 17 June 2013, Accepted 20 July 2013, Scheduled 26 July 2013*

\* Corresponding author: Hang Zhou (zh\_cn1120@163.com).

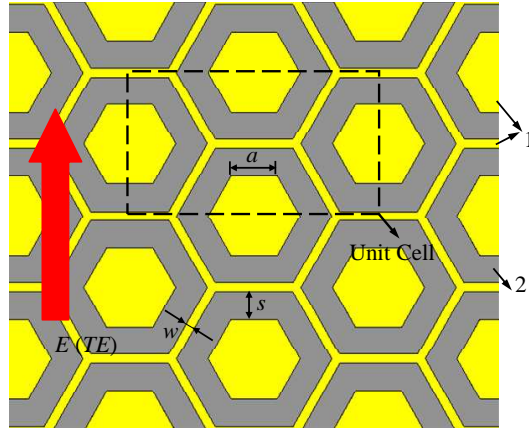
80 degree. Consequently, in order to reduce the RCS of radar in the out-band of FSS, and meanwhile to ensure normal communications of the airplane, a bandpass FSS with stable performance under large incident angles is required. However, to achieve this target is not easy, even for a thin FSS structure. Munk and Luebbers studied the effects of dielectric loadings on FSSs. When the dielectric slabs with a thickness of about  $0.3\lambda$  and  $\epsilon_r \sim 1.5$  are added on the surface of FSS, the bandpass stability under large incident angles is greatly improved [1,6]. However, this method would make the FSS bulky, and thus is limited to some applications. A streamlined metallic FSS radome was designed in [4] using arrays of slots etched into a solid thin metal curved radome. The radome permits transmission with any polarization over a wide range of scan angles. Since then, for about four decades, many researchers have been dedicated to designing novel FSS structures with stable performance. Three-dimensional FSS structures were designed to obtain isotropic performances [7]. Complementary FSSs have been proposed in [8, 9]. Miniaturized FSS, whose dimensions are much smaller than the operating wavelength, were investigated in [10, 11]. FSSs with very small unit cell dimensions have been proposed in [12–15]. To achieve high  $Q$ -factor from open resonators, substrate integrated waveguide (SIW) technology was introduced by Luo et al. [16, 17] to design high-performance FSS.

In this paper, we propose a novel FSS with stable performance. It is composed of hexagon metallic lines and hexagon patches. Such a FSS has the merits of compactness, low profile, and stable performance under large incident angles.

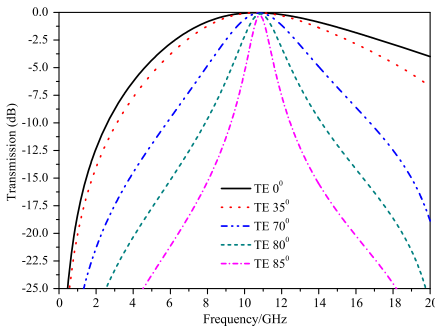
## 2. DESIGN AND ANALYSIS

Figure 1 shows the top view of the FSS structure, which has only a metallic layer on a dielectric substrate. The metallic structure is composed of hexagon metallic lines and hexagon patches. The back of the substrate has no metallic structures. Dimensions of the structure are  $a = 3.0$  mm,  $s = 1.2$  mm,  $w = 0.2$  mm. The FSS uses a F4B-2 substrate with a relative permittivity of  $\epsilon_r = 2.65$ , a loss tangent of 0.001 and a thickness of  $h = 0.6$  mm.

We use CST Microwave Studio to calculate its transmission characteristics. The four sides of the unit cell are set to be periodic boundary conditions (PBC). The unit cell is excited by an incident plane wave with different incident angles and polarizations. For  $TE$  polarization, the  $E$  field direction is shown in Figure 1. Figure 2 and Figure 3 give the transmission responses under different incidence angles and polarizations. Under normal incidence, it can be found



**Figure 1.** Front view of the proposed FSS structure. The FSS is a single-layer structure with no metallic structure on the back of the substrate.  $a = 3.0$  mm,  $w = 0.2$  mm,  $s = 1.2$  mm. 1. Metallic structure. 2. F4B-2 substrate, whose permittivity is 2.65, loss tangent is 0.001 and thickness is 0.6 mm.



**Figure 2.** Transmission responses under different incidence angles for *TE* polarization.

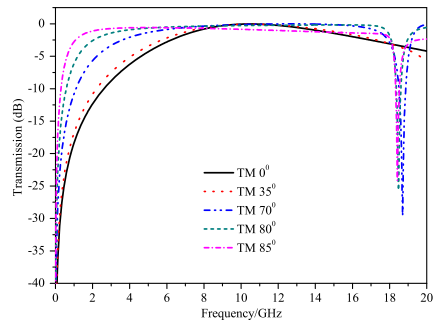


**Figure 3.** Transmission responses under different incidence angles for *TM* polarization.

that a resonance transmission pole response occurs at about 10.62 GHz.  $-1$  dB bandwidth of the passband is 6.74 GHz (7.42–14.16 GHz). From Figure 2 we can observe that for *TE* polarization, bandwidths of the passband become narrower as the incident angles increase. However, resonance of the transmission is rather stable even when the incident angle comes to  $85^\circ$ .  $-1$  dB bandwidths of the passband are 1.17 GHz (10.12–11.29 GHz) and 0.48 GHz (10.58 to 11.06 GHz) for  $80^\circ$  and  $85^\circ$

incident angles, respectively.

For *TM* polarization, as shown in Figure 3, bandwidths of the passband become wider as the incident angles increase. In the passband, from 10.12 to 11.29 GHz, insertion losses are below 1 dB. Figure 4 shows the field distribution on the surface of the FSS at 10.62 GHz with (a) electric field and (b) surface current. It can be observed that a resonance occurred on the hexagon patches surrounded by the metallic lines. And there is a surface current flow through the metallic lines. Accordingly, the passband arise from enhanced transmission assisted by the metallic line and the patches.

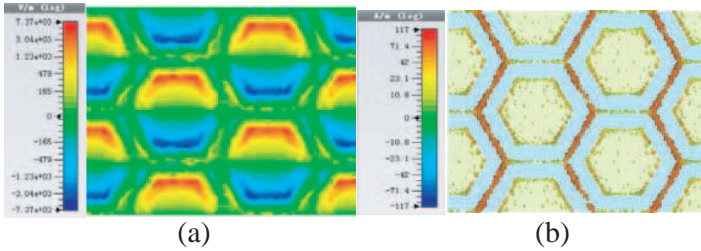


**Figure 4.** Field distribution diagrams at 10.62 GHz. (a) Electric field. (b) Surface current.

### 3. EXPERIMENT

An experiment was implemented to verify our design. The designed FSS was fabricated by printed circuit board (PCB) technology using a F4B-2 substrate, whose permittivity is 2.65, loss tangent 0.001 and with the thickness of 0.6 mm. Figure 5 shows the prototype of the fabricated structure. It is made up of an array of  $22 \times 38$  unit cells, so the overall size of the structure is 297 mm  $\times$  296.2 mm. A free space measurement system composed of two horn antennas (one is the transmitter, the other one is the receiver), a vector network analyzer and a test fixture was used to measure the FSS structure. A pair of wideband horn antennas operating in 1.0–18.0 GHz is used to implement this experiment. Hence, the measurement frequency range of the experiment is from 1.0 GHz to 18.0 GHz.

Measured transmission results under normal incidence, plus a comparison with the simulation ones, is shown in Figure 6. We can observe from Figure 6 that the measured results have the same trend with the simulation ones. The reason of the ripples arise in the measured results is due to that the sample is not large enough and edge diffractions will lead to the ripples of the measured results. Especially,

at lower frequencies, the measured transmission levels are likely to be perturbed by scattered signals [12]. Limited by the size of the sample, the incident angles in the measurement is limited below  $45^\circ$ . Figure 7 and Figure 8 show the experimental results versus simulation ones for  $TE\ 45^\circ$  and  $TM\ 45^\circ$ , respectively. In addition, we use another pair of horn antennas whose scales are smaller, and their operating frequencies are 10.0–18.0 GHz. In these frequencies band, the incident angles can be measured to  $70^\circ$ . Figure 9 shows the experimental results versus simulation ones for  $TE\ 70^\circ$ . The measured results agree well with the simulation ones no matter how the polarization and the incident angles are changed. From the measured results, it can be concluded that although the measured results are not perfect compared with the simulation ones, they still can prove our design.

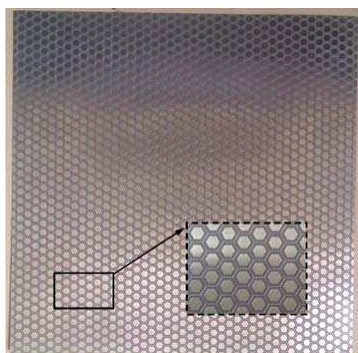


**Figure 5.** Prototype of the fabricated structure.

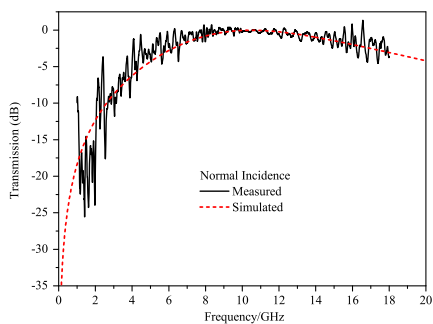


**Figure 6.** Experimental results versus simulation ones for normal incidence.

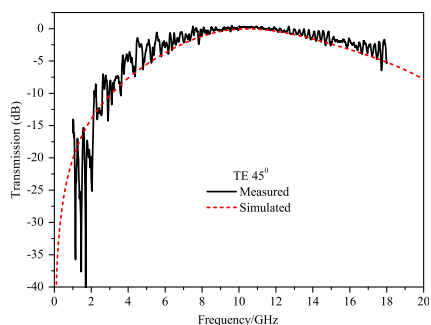


**Figure 7.** Experimental results versus simulation ones for  $TE\ 45^\circ$ .

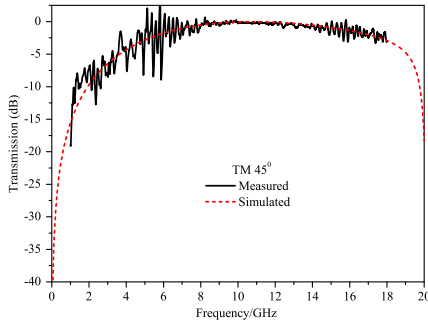


**Figure 8.** Experimental results versus simulation ones for  $TM$   $45^\circ$ .

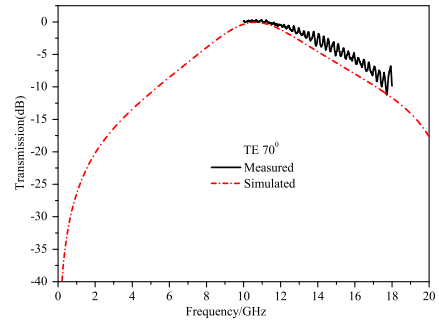


**Figure 9.** Experimental results versus simulation ones for  $TE$   $70^\circ$ .

#### 4. CONCLUSION

In this paper, we propose a novel FSS with stable performance under larger incident angles. It is composed of hexagon metallic lines and hexagon patches. Both the simulation and experimental results show that the proposed FSS has advantages of stable performances, low insertion losses under large incident angles. Moreover, its thickness is about  $\lambda/47$  for the central frequency passband. The presented FSS provides practical applications for airborne FSS radome.

#### ACKNOWLEDGMENT

This work was supported Project supported by the National Natural Science Foundation of China (Grant Nos. 61202339, 61203268) and in part by the Natural Science Foundation of Shaanxi Province of China under Grant No. 2012JQ8034 and partly by the Postdoctoral Science Foundation of China (Grant No. 2012M512144).

#### REFERENCES

1. Munk, B. A., *Frequency Selective Surfaces: Theory and Design*, Wiley, New York, 2000.
2. Yuan, Y., H. Zhou, X.-H. Wang, and Y. Mi, "Low-pass frequency selective surface with wideband high-stop response for shipboard radar," *Journal of Electromagnetic Waves and Applications*, Vol. 27, No. 1, 117–122, 2013.

3. Martinez-Lopez, R., J. Rodriguez-Cuevas, A. E. Martynyuk, and J. I. Martinez Lopez, "An active ring slot with RF MEMs switchable radial stubs for reconfigurable frequency selective surface applications," *Progress In Electromagnetics Research*, Vol. 128, 419–440, 2012.
4. Pelton, E. L. and B. A. Munk, "A streamlined metallic radome," *IEEE Trans. Antennas Propag.*, Vol. 22, No. 6, 799–803, Nov. 1974.
5. Zhou, H., S. Qu, B. Lin, J. Wang, H. Ma, and Z. Xu, "Filter-antenna consisting of conical FSS radome and monopole antenna," *IEEE Trans. Antennas Propag.*, Vol. 60, No. 6, 3040–3045, 2012.
6. Luebbers, R. J. and B. A. Munk, "Some effects of dielectric loading on periodic slot arrays," *IEEE Trans. Antennas Propag.*, Vol. 26, No. 4, 536–542, 1978.
7. Baena, J. D., L. Jelinek, R. Marqués, J. J. Mock, J. Gollub, and D. R. Smith, "Isotropic frequency selective surfaces made of cubic resonators," *Appl. Phys. Lett.*, Vol. 91, No. 19, 191105, 2007.
8. Wakabayashi, H., M. Kominami, H. Kusaka, and H. Nakashima, "Numerical simulations for frequency-selective screens with complementary elements," *IEE Pro. — Micro. Antennas Propag.*, Vol. 141, No. 6, 477–482, 1994.
9. Lockyer, D. S., J. C. Vardaxoglou, and R. A. Simpkin, "Complementary frequency selective surfaces," *IEE Pro. — Micro. Antennas Propag.*, Vol. 147, No. 6, 501–507, 2000.
10. Sarabandi, K. and N. Behdad, "A frequency selective surface with miniaturized elements," *IEEE Trans. Antennas Propag.*, Vol. 55, No. 5, 1239–1245, 2007.
11. Bayatpur, F. and K. Sarabandi, "Miniaturized FSS and patch antenna array coupling for angle-independent, high-order spatial filtering," *IEEE Microw. Wireless Compon. Lett.*, Vol. 20, No. 2, 79–81, 2010.
12. Moallem, M. and K. Sarabandi, "Miniaturized-element frequency selective surfaces for millimeter-wave to Terahertz applications," *IEEE Trans. Terahertz Science Tech.*, Vol. 2, No. 3, 333–339, 2012.
13. Parker, E. A. and A. N. A. El Sheikh, "Convolutd array elements and reduced size unit cells for frequency selective," *IEE Pro. — Micro. Antennas Propag.*, Vol. 138, No. 1, 19–22, 1991.
14. Sanz-lzquierdo, B., E. A. Parker, J.-B. Roberson, and J. C. Batchelor, "Singly and dual polarized convolutd frequency selective structures," *IEEE Trans. Antennas Propag.*, Vol. 58, No. 3, 690–696, 2010.

15. Zheng, S. F., Y. Z. Yin, H. L. Zheng, Z. Y. Liu, and A. F. Sun, "Convolutated and interdigitated hexagon loop unit cells for frequency selective surfaces," *Electron. Lett.*, Vol. 47. No. 4, 233–235, 2011.
16. Luo, G. Q., W. Hong, Z. C. Hao, B. Liu, W. D. Li, et al., "Theory and experiment of novel frequency selective surface based on substrate integrated waveguide technology," *IEEE Trans. Antennas Propag.*, Vol. 53, No. 12, 4035–4043, Dec. 2005.
17. Luo, G. Q., W. Hong, Q. H. Lai, K. Wu, and L. L. Sun, "Design and experimental verification of compact frequency-selective surface with quasi-elliptic bandpass response," *IEEE Trans. Microw. Theory Tech.*, Vol. 55, No. 12, 2481–2487, 2007.